IAEA-SM-174/12

LA-UR -73-999

Conf-730823--6

TITLE: MODIFIED DEFINITION OF THE SURFACE ENERGY IN THE LIQUID-DROP FORMULA

AUTHOR(S): H. J. Krappe and J. R. Nix

SUBMITTED TO: Third IAEA Symposium on the Chemistry and Physics of Fission, Rochester, New York, August 13-17, 1973

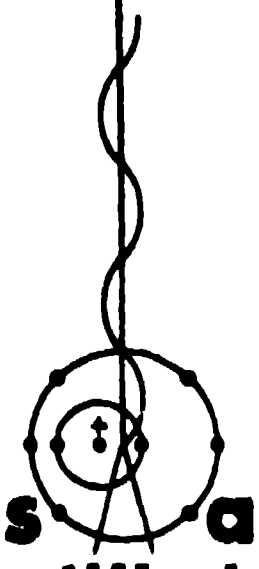

los alamos
scientific laboratory
of the University of California
LOS ALAMOS, NEW MEXICO 87544

UNITED STATES
ATOMIC ENERGY COMMISSION
CONTRACT W-7405-ENG. 36

IAEA-SM-174/12

MODIFIED DEFINITION OF THE SURFACE ENERGY IN THE LIQUID-DROP FORMULA*

H. J. Krappe†

Lawrence Berkeley Laboratory
University of California
Berkeley, California 94720 U.S.A.

and

J. R. Nix

Los Alamos Scientific Laboratory
University of California
Los Alamos, New Mexico 87544 U.S.A.

ABSTRACT

When calculated in the liquid-drop model, the deformation energy of strongly necked-in fission or fusion configurations shows a spuriously strong dependence on the details of the shape in the neck region. This is a consequence of the assumed sharp surface in the liquid-drop model. This model can be improved by replacing the surface-energy term by the self-energy of a drop caused by a short-range two-particle interaction. For a Yukawa function the self-energy integral can be evaluated analytically for a few important special configurations, and it can be transformed into a three-dimensional integral for arbitrary axially symmetric shapes. A numerical calculation is therefore only slightly more complicated than the usual treatment of the Coulomb energy.

---

*This work was supported by the U. S. Atomic Energy Commission and the German Academic Exchange Service

†Hahn-Meitner Institut für Kernforschung, Berlin, Federal Republic of Germany. Visitor to the Lawrence Berkeley Laboratory, April 1972-September 1973.

In addition to the parameters in the conventional liquid-drop model, the new definition of the nuclear part of the deformation energy contains a parameter to specify the range of the Yukawa function. Parameters for the new definition are determined from fission-barrier heights and interaction-barrier heights throughout the periodic table.

The influence of the proposed change in the liquid-drop formula on the stiffness of spherical nuclei, the ground-state deformation, and the existence of shape isomeric states in light nuclei is discussed. Fission-barrier heights and saddle-point shapes are determined for nuclei along the line of beta-stability, and the static interaction potential between heavy ions is calculated.

1. INTRODUCTION

Considerable progress has been made in calculating the nuclear potential energy of deformation as a function of the nuclear shape and the mass and charge numbers by splitting it into a slowly varying function of these quantities and a rapidly fluctuating part. The latter is usually calculated according to a prescription given by Strutinsky [1]. Here we will deal only with the smooth part. It is usually expressed in terms of a Bethe-Weizsacker type of expansion in powers of $A^{-1/3}$ and I^2, for example [2-4]

$$E_{LD} = -C_v A + C_s A^{2/3} B_s(\xi_\nu) + \frac{3}{5}\frac{e^2 Z^2}{r_0 A^{1/3}}\left[B_c(\xi_\nu) - \frac{5}{6}\pi^2 \frac{d^2}{r_0^2 A^{2/3}} - \frac{0.7636}{Z^{2/3}}\right], \quad (1)$$

where

$$C_v = a_v(1 - \kappa_v I^2) \quad ,$$

$$C_s = a_s(1 - \kappa_s I^2) \quad ,$$

and

$$I = (N - Z)/A.$$

The quantity d is the surface-thickness parameter in a Fermi function that specifies the charge distribution. The shape-dependent function $B_s(\xi_\nu)$ is the ratio of the surface area of the deformed nucleus to that of the spherical nucleus, and $B_c(\xi_\nu)$ is the ratio of the Coulomb energy of the deformed equivalent sharp-surface nucleus to that of the spherical nucleus. Such a leptodermous expansion is valid only if all geometrical dimensions of the drop are large compared to the surface thickness. This condition is not satisfied for strongly necked-in configurations with neck radii smaller than about 2 fm, for example around the scission region in fission or the point of first contact in heavy-ion reactions.

One could overcome this difficulty by going back to a constrained self-consistent microscopic calculation for such configurations. But that would be a rather involved program from a numerical point of view. Therefore, it is desirable to construct a generalization of the liquid-drop formula - still on a purely phenomenological basis - which satisfies the following conditions:

(1) For spherical configurations it should give practically the same result as the old liquid-drop formula (except for very light nuclei).

(2) In contrast to the usual surface energy it should not be sensitive to high-multipole wiggles on the surface of the drop. The liquid-drop formula yields a spurious and undesirable sensitivity of calculated fission barriers on unphysical fine details of the shape in the neck region.

(3) Between two separated fragments there should be an attractive nuclear interaction energy besides the Coulomb repulsion. The range of that force should extend beyond the equivalent sharp radius by roughly the range of the nucleon-nucleon interaction.

(4) It should be possible to calculate the new expression for general shapes with reasonable computational effort.

We will show that one can satisfy these conditions by replacing the surface energy term $C_s\, A^{2/3}\, B_s(\xi_\nu)$ by

$$E = -\frac{V_0}{4\pi a^3} \int d^3r\, d^3r' \, \frac{e^{-\frac{|\vec{r}-\vec{r}'|}{a}}}{\frac{|\vec{r}-\vec{r}'|}{a}} \quad , \tag{2}$$

with the two phenomenological parameters V_0 and a instead of the single liquid-drop parameter C_s and allowing for a renormalization of the volume-energy coefficient C_v. The six-fold integral is to be taken over the volume of the equivalent sharp-surface nucleus whose shape can be parametrized by any suitable set of deformation parameters; this volume is specified by the nuclear-radius parameter r_0.

2. SPECIAL CONFIGURATIONS

We will discuss the results of this replacement for a sequence of shapes of increasing complexity and show that these four conditions are fulfilled.

2.1. Spherical shape

A straightforward calculation of the integral (2) in spherical coordinates yields

$$E = V_0\left[-\frac{4\pi}{3}R_0^3 + 2\pi a R_0^2 - 2\pi a^3 + 2\pi a(R_0 + a)^2\, e^{-2R_0/a}\right] \quad ,$$

where $R_0 = r_0 A^{1/3}$ is the equivalent sharp radius. For $a/R_0 \ll 1$ the last two terms are negligible. The second term yields the surface energy if the interaction strength V_0 is related to the semi-empirical surface-energy constant C_s by

$$C_s = a_s(1 - \kappa_s I^2) = 2\pi V_0 a\, r_0^2 \quad .$$

The first term gives a contribution to the volume energy and has to be compensated for by a renormalization of C_v. This way we meet the first of the four requirements on E. The limit $a \to 0$ yields the usual liquid-drop model.

2.2. Bubble nucleus

For a bubble nucleus with inner radius R_1 and outer radius R_2 one gets from (2)

$$E = -\left(\frac{a}{r_0}\right)^2 C_s \left[\frac{2}{3}\left(\frac{R_2}{a}\right)^3 - \frac{2}{3}\left(\frac{R_1}{a}\right)^3 - \left(\frac{R_2}{a}\right)^2 - \left(\frac{R_1}{a}\right)^2 + 2 - \left(\frac{R_1}{a}+1\right)^2 \exp(-2R_1/a)\right.$$

$$+ 2\left(\frac{R_1}{a}-1\right)\left(\frac{R_2}{a}+1\right)\exp\left(-\frac{R_2-R_1}{a}\right) + 2\left(\frac{R_1}{a}+1\right)\left(\frac{R_2}{a}+1\right)\exp\left(-\frac{R_1+R_2}{a}\right)$$

$$\left. - \left(\frac{R_2}{a}+1\right)^2 \exp(-2R_2/a)\right] \quad .$$

Recently the bubble-nucleus model has been discussed for $R_1 \approx a$ [5]. In this case the application of the usual liquid-drop formula (1) is doubtful and should be replaced by this formula.

2.3. Small distortions about a spherical shape

If the shape is parametrized by the normal coordinates for harmonic vibrations around the spherical shape,

$$R = R_0 \left(1 + \sum_{\substack{l \geq 2 \\ m}} \beta_{lm} Y_{lm}(\Omega) + \beta_{corr}\right) \quad , \qquad (3)$$

where

$$\beta_{corr} = -\frac{1}{4\pi} \sum_{\substack{l \geq 2 \\ m}} |\beta_{lm}|^2 \quad ,$$

the deformation energy to second order in β_{lm} is given by

$$E(\beta_{lm}) - E(0) = \frac{C_s}{4\pi} A^{2/3} \sum_{\substack{l \geq 2 \\ m}} |\beta_{lm}|^2 C_l \quad , \qquad (4)$$

where

$$C_\ell = \left(\frac{R_0}{a}+1\right)\left[\frac{R_0}{a}-1+\left(\frac{R_0}{a}+1\right)\exp(-2R_0/a)\right] - 2\left(\frac{R_0}{a}\right)^3 I_{\ell+1/2}\left(\frac{R_0}{a}\right)K_{\ell+1/2}\left(\frac{R_0}{a}\right) .$$

Here $I_{\ell+1/2}$ and $K_{\ell+1/2}$ are modified Bessel and Hankel functions, respectively [6].

The simplest way to derive this formula is to use the expansion

$$\int d\Omega \int_0^{R(\Omega)} r^2 f(|\vec{r}-\vec{r}'|)\, dr = \int d\Omega \left[\int_0^{R_0} r^2 f(|\vec{r}-\vec{r}'|)\, dr + R_0^3 f(|\vec{r}-\vec{r}'|)_{r=R_0}\left(\sum_{\ell,m}\beta_{\ell m} Y_{\ell m}(\Omega) + \beta_{corr}\right)\right. \quad (5)$$

$$\left. + \frac{R_0^2}{2}\frac{\partial}{\partial r} r^2 f(|\vec{r}-\vec{r}'|)_{r=R_0}\left(\sum_{\ell,m}\beta_{\ell m} Y_{\ell m}(\Omega)\right)^2\right]$$

for the integration with respect to r and a similar one for the integration with respect to r'. Integrals of the type

$$\int_{-1}^{1} dx\, P_\ell(x)\, \frac{\exp\left(-\frac{1}{a}\sqrt{r_1^2+r_2^2-2r_1r_2x}\right)}{\frac{1}{a}\sqrt{r_1^2+r_2^2-2r_1r_2x}}$$

are evaluated by use of the addition theorem for modified Bessel functions [6],

$$\frac{\exp\left(-\frac{1}{a}\sqrt{r_1^2+r_2^2-2r_1r_2x}\right)}{\frac{1}{a}\sqrt{r_1^2+r_2^2-2r_1r_2x}} = \sum_{\ell=0}^{\infty}(2\ell+1)\, P_\ell(x)\, \frac{a}{\sqrt{r_1r_2}} I_{\ell+1/2}\left(\frac{r_1}{a}\right)K_{\ell+1/2}\left(\frac{r_2}{a}\right) . \quad (6)$$

An expansion of Eq. (4) in powers of $A^{-1/3}$ yields for the stiffness constant for multipole vibrations of order ℓ the result

$$\frac{C_s}{4\pi} A^{2/3} C_\ell = \frac{C_s}{8\pi} \left\{ [\ell(\ell+1)-2]A^{2/3} - \frac{3}{4}(\ell-1)\ell\ (\ell+1)\ (\ell+2) \left(\frac{a}{r_0}\right)^2 \right\}$$

$$+ \sigma \left(\frac{a^4}{r_0^4} A^{-2/3} \right) + \sigma\ [\exp\ (-2R_0/a)] \quad .$$

The first term is the well-known contribution of the surface energy in the liquid-drop formula. There is no term proportional to $A^{1/3}$, which means physically that the contribution to the energy from the curvature of the nuclear surface is identically zero. This $A^{1/3}$ term is absent also for more general shapes [7], provided that the smallest curvature radius is large compared to the range a. The term of order A^0 reduces the stiffness for finite values of the range a; this reduction becomes relatively more important for light nuclei. The last two terms are negligible for low multipole orders ℓ, provided that the nuclear radius R_0 is large compared to a. For higher multipoles, the expression (4) for the stiffness constant becomes independent of multipole order, because for large ν

$$I_\nu(z)\ K_\nu(z) \longrightarrow \frac{1}{2\nu} \quad .$$

This is to be contrasted to the quadratic increase with multipole order for the stiffness constant calculated with the usual liquid-drop model. It shows the insensitivity of the modified liquid-drop formula to unphysical fine wiggles of the surface. Therefore also the second of the four requirements on E is satisfied by (2).

The fissility parameter x is defined as the ratio of the Coulomb energy $E_c^{(0)}$ of a spherical sharp-surface drop to twice the spherical surface energy $E_s^{(0)} = C_s \cdot A^{2/3}$. The value of the critical fissility x_{crit} for which the sphere loses stability against fission corresponds to the point where the restoring force aginnst P_2 vibrations vanishes. Addition of the Coulomb contribution to the deformation energy (4) yields for $\ell=2$, $m=0$ the result

$$\delta E = \frac{E_s^{(0)}}{4\pi}\ \beta_{20}^2\ \left[2 - 2x - 9\frac{a^2}{R_0^2} + \sigma\ (e^{-2R_0/a}) \right] \quad .$$

This leads to

$$x_{crit} = 1 - \frac{9}{2}\left(\frac{a}{R_0}\right)^2 + \sigma\ (e^{-2R_0/a}) \qquad (7)$$

instead of the usual value 1.

2.4. Two non-overlapping spheres

The nuclear interaction energy of two non-overlapping spheres of radii R_1 and R_2 and center-of-mass distance $D \geq R_1 + R_2$ follows from straight-forward integration of (2):

$$E_{int} = - 4 \left(\frac{a}{r_0}\right)^2 C_s \left(\frac{R_1}{a} \cosh \frac{R_1}{a} - \sinh \frac{R_1}{a}\right) \left(\frac{R_2}{a} \cosh \frac{R_2}{a} - \sinh \frac{R_2}{a}\right) \frac{e^{-D/a}}{D/a} . \quad (8)$$

For $R_{1,2}/a \gg 1$ this reduces to

$$E_{int} = - 4 \pi \gamma \frac{R_1 R_2}{R_1+R_2} \, a e^{-\ell/a} + \mathcal{O}\left(\frac{a}{R_1}, \frac{a}{R_2}, \frac{\ell}{R_1+R_2}\right) ,$$

where ℓ is the distance between the two sharp surfaces and $\gamma = \frac{C_s}{4\pi r_0^2}$ is the surface tension.

This formula is a special case of a general theorem [8] which states that to order $\frac{a}{R}$ the interaction energy between two arbitrarily shaped objects interacting via a short range force (short compared to all curvature radii) can always be expressed in the form

$$E_{int}(\ell) = \frac{2\pi}{\sqrt{D_{xx} D_{yy}}} \int_\ell^\infty e(\xi) \, d\xi + \mathcal{O}\left(\frac{a}{R}\right) .$$

The first factor is purely geometrical and in the case of two spheres is equal to $2\pi R_1 R_2/(R_1+R_2)$. The quantity $e(\xi)$ is the interaction energy per unit area of two parallel infinite surfaces at distance ξ. Obviously $e(0) = - 2\gamma$. A Thomas-Fermi calculation [8] of the function $e(\xi)$ yields a result that can be approximated roughly by an exponential function of range $a = 1.4$ fm, that is,

$$e(\xi) \approx - 2 \gamma \, e^{-\xi/(1.4 \text{ fm})} .$$

2.5. Non-overlapping spherical nucleus and slightly deformed nucleus

The generalization of Eq. (8) to the interaction energy between a spherical nucleus with radius R_1 and a deformed nucleus with radius $R = R_2 \left[1 + \beta_{corr} + \sum_{\ell,m} \beta_{\ell m} Y_{\ell m}(\Omega)\right]$ is given to second order in $\beta_{\ell m}$ by

$$E_{int} - E_{int}^{sph} = -2C_s\left(\frac{a}{r_0}\right)^2 \left(\frac{R_1}{a}\cosh\frac{R_1}{\varepsilon} - \sinh\frac{R_1}{a}\right)\left(\frac{R_2}{a}\right)^3 \tag{9}$$

$$\times\left[\sum_{\ell,m}\sqrt{\frac{4\pi}{2\ell+1}}\,Y_{\ell m}(0,\psi)\left(\beta_{\ell m}\,A_\ell + \sum_{\ell',\ell'',m'}\beta_{\ell' m'}\beta_{\ell'' m-m'}\,C_{\ell,\ell',\ell'',m,m'}\right)\right].$$

Here θ and ψ are the angular coordinates of the body-fixed coordinate system of the deformed nucleus relative to the vector joining the centers of mass of the two nuclei. The deformation parameters $\beta_{\ell m}$ refer to the body-fixed system. The other quantities are given by

$$A_\ell = \sqrt{\frac{2\ell+1}{\pi}}\,\frac{a}{\sqrt{R_2 D}}\,I_{\ell+1/2}\left(\frac{R_2}{a}\right)\,K_{\ell+1/2}\left(\frac{D}{a}\right) \quad ,$$

$$C_{\ell,\ell',\ell'',m,m'} = \left[\frac{(2\ell'+1)(2\ell''+1)}{4\pi(2\ell+1)}\right]^{1/2}(\ell' m' \ell'' m-m' | \ell m)(\ell' 0 \ell'' 0 | \ell 0)\,\frac{1}{2R_2}\,\frac{\partial}{\partial R_2}\,(R_2^2 A_\ell) \quad ,$$

$$\beta_{00} = \sqrt{4\pi}\,\beta_{corr} \quad ,$$

and E_{int}^{sph} is the expression (8) for the spherical case. This formula is obtained easily by use of the expansions (5) and (6).

3. DETERMINATION OF PARAMETERS

The shape-dependent terms of the nuclear macroscopic energy calculated according to Eq. (1) contain a total of four parameters: the equivalent sharp-surface nuclear-radius parameter r_0, the range a of the Yukawa function, the surface-energy constant a_s for equal numbers of neutrons and protons, and the surface-asymmetry constant κ_s. The equivalent sharp-surface nuclear-radius parameter r_0 is known accurately from analyses of electron-scattering data; its value is therefore not adjusted but is taken instead to be 1.16 fm from these studies [9].

Interaction-barrier heights depend mainly on r_0 and the range a and more weakly on a_s and κ_s. Therefore, once r_0 is fixed the range a is determined by adjusting to experimental interaction-barrier heights [10-25]. The resulting value of 1.4 fm is the same as the range determined from the above mentioned Thomas-Fermi calculations [8].

Once both r_0 and a are known, the final two parameters a_s and κ_s are determined by adjusting to experimental fission-barrier heights [26-28].

Because these two parameters are highly correlated, their individual values are determined poorly. For example, the value of 4.0 determined for κ_s is uncertain by at least ± 1.0.

The resulting value of 24.7 MeV for a_s is significantly higher than the value of about 18 MeV obtained in the usual liquid-drop model by adjusting to fission barrier heights [2,3]. It is on the other hand only slightly larger than values obtained by adjusting to nuclear ground-state masses alone [4]. The difference between our value and the values of Refs. [2,3] arises because the finite range of the nuclear force reduces the effective stiffness with respect to deformations. It is therefore possible that the surface-energy constant is indeed larger than previously believed.

To summarize, the preliminary values chosen for the four parameters are

$$\left.\begin{aligned} r_0 &= 1.16 \text{ fm} \quad , \\ a &= 1.4 \text{ fm} \quad , \\ a_s &= 24.7 \text{ MeV} \quad , \\ \kappa_s &= 4.0 \quad . \end{aligned}\right\} \tag{10}$$

No attempt has been made so far to redetermine the parameters in the shape-independent terms of Eq. (1) after replacing the surface term by the integral (2).

4. INTERACTION BARRIERS

The combined action of the Coulomb and the nuclear force usually yields a maximum in the interaction-energy as a function of the distance between two ions. For symmetric configurations this interaction barrier disappears for a critical fissility of the combined system of $x = 6/5$, at which point the Coulomb repulsion can no longer be counter-balanced by the nuclear force even for two touching spheres. Below this critical value of x the height of the barrier is often represented in the form

$$E_{int}^{max} = \frac{Z_1 Z_2 e^2}{r_{eff}(A_1^{1/3} + A_2^{1/3})} \quad . \tag{11}$$

Figure 1 shows r_{eff} as a function of the charges Z_1 and Z_2 of the two colliding ions for nuclei along Green's approximation to the line of beta-stability [29]. Equation (11) can be rewritten in the form

$$E_{int}^{max} = \frac{Z_1 Z_2 e^2}{R_1 + R_2 + a + d} \quad , \tag{12}$$

where d is the distance between the two nuclear surfaces at which the total interaction energy has its maximum. The value of d is determined easily by iteration from the equations

$$\frac{d}{dD}\left(\frac{e^2 Z_1 Z_2}{D} + E_{int}(D)\right)\Bigg| = 0 \quad ,$$

$$D = r_0(A_1^{1/3} + A_2^{1/3}) + d \quad ,$$

where $E_{int}(D)$ is inserted from Eq. (8). A contour plot of $d(Z_1,Z_2)$ for nuclei along the line of beta-stability is given in Fig. 2.

In Fig. 3 experimental Coulomb barriers from reaction cross-section measurements [10-18] and from elastic scattering experiments are compared with the predictions of this theory. The deviations from the calculated values are smaller than ± 5.4% or 9 MeV in absolute units. The data used in Fig. 3 include the deformed nuclei ^{238}U [13-15,19], ^{232}Th [10], and ^{164}Dy [12]. For these deformed nuclei Eq. (9) is used with $\beta_{20} = 0.277$, 0.248, and 0.319, respectively [30]. The orientation angles θ and ψ are taken equal to zero, which gives the minimum interaction barrier. We have not taken into account any shell effects on interaction barriers because the influence of one potential well on the level density around the Fermi surface in the other well is supposed to be very small at the point of geometrical contact or even farther out.

The distance between the two centers of mass is the only degree of freedom that we have considered in calculating interaction barriers. We are thus disregarding the coupling of the relative motion to the neck-healing or any intrinsic degrees of freedom of the two ions. Elastic-scattering data on the other hand are usually analyzed in terms of optical potentials. Only the tail regions of these potentials are determined unambiguously, which often excludes the maximum. Moreover the optical potential reflects the coupling of intrinsic degrees of freedom to the relative motion in an average way, whereas these effects are completely neglected in our model.

Information on interaction barriers is also extracted from fusion reaction cross sections. They are mostly analyzed in terms of transmission coefficients calculated by assuming transmission of a real parabolic potential barrier. This amounts to assuming an ingoing-wave boundary condition inside the potential barrier. It has been shown [31] that optical-model potentials are not necessarily identical with potentials to be used with an ingoing-wave boundary condition, especially when the imaginary part is neglected or not determined in the latter method.

To overcome the problems connected with the ambiguity in potential fits it is advisable to determine the critical angular momentum $\Lambda(E)$ as a function of energy from a phase-shift analysis of elastic or reaction scattering data [32]. Using the relation

$$\Lambda(\Lambda+1) = (kR_r)^2 \left(1 - \frac{V(R_r)}{E}\right)$$

for several energies, one can extract the pair of values $V(R_r)$ and R_r, i.e. the interaction potential at the reaction radius R_r, independent of where the maximum of that potential might be. Of course, the assumption has been made that the interaction can be described by an energy-independent, local potential and that the process is purely diffractive.

5. GENERAL SHAPES

The integral (2) can be reduced to the double surface integral

$$E = \frac{V_0 a}{4\pi} \int\int d\vec{S} \cdot (\vec{r}-\vec{r}')\, d\vec{S} \cdot (\vec{r}-\vec{r}') \left[\frac{|\vec{r}-\vec{r}'|}{a} + \left(2 + \frac{|\vec{r}-\vec{r}'|}{a}\right) e^{-\frac{|\vec{r}-\vec{r}'|}{a}} - 2\right] \times |\vec{r}-\vec{r}'|^{-4} \tag{13}$$

by using the identity

$$\vec{\nabla}_r \cdot (\vec{r}-\vec{r}')\, \vec{\nabla}_{r'} \cdot (\vec{r}-\vec{r}') \left[\frac{|\vec{r}-\vec{r}'|}{a} + \left(2 + \frac{|\vec{r}-\vec{r}'|}{a}\right) e^{-\frac{|r-r'|}{a}} - 2\right] \left(\frac{|\vec{r}-\vec{r}'|}{a}\right)^{-4}$$

$$= -\frac{e^{-\frac{|\vec{r}-\vec{r}'|}{a}}}{\frac{|\vec{r}-\vec{r}'|}{a}}$$

and applying Gauss's theorem with respect to $\vec{r}$ and $\vec{r}'$. For systems with cylindrical symmetry (13) reduces to the three-dimensional integral in cylindrical coordinates

$$E = -\frac{V_0}{2a^3} \int dz \int dz' \int_0^{2\pi} d\psi\, R(z) \left[R(z) - R(z') \cos\psi - R'(z)(z-z')\right] R(z') \times \left[R(z') - R(z) \cos\psi - R'(z')(z'-z)\right] \frac{\left[d + (2+d)e^{-d} - 2\right]}{d^4}, \tag{14}$$

where

$$d = \frac{1}{a}\left[R^2(z) + R^2(z') - 2R(z)\,R(z')\cos\psi + z^2 + z'^2 - 2zz'\right]^{1/2} \quad .$$

The function R(z) gives the shape in cylindrical coordinates, and R'(z) is the derivative of R(z) with respect to z. The z integrations are taken between the zeros of R(z). The three-fold integral (14) in general must be evaluated numerically, but this is only slightly more complicated than the evaluation of the integral for the Coulomb energy.

6. FISSION BARRIERS

Figure 4 shows the maximum and minimum radii of saddle-point shapes as functions of the fissility parameter x for various values of the range a. The remaining constants are held fixed at the values determined in Ref. [3] on the basis of the liquid-drop model, that is, for zero range. The saddle points are calculated by use of the methods of Ref. [33], with the surface energy replaced by Eq. (14). The class of shapes investigated is that of two spheroids connected smoothly by a quadratic surface of revolution [33]. There is a clear tendency to more compact saddle-point shapes with increasing a for fixed values of the other constants. The shift of x_{crit} to values smaller than 1 as given by (7) to second order in $\frac{a}{R_0}$ is also clearly seen. The critical Businaro-Gallone point (where stability against mass asymmetry is lost) [34] first moves to slightly larger values of the fissility x with increasing range a. It reaches a maximum at $a/r_0 \approx 0.7$ and then it moves back to smaller values of x. Figure 5 gives the fission-barrier height as a function of the fissility parameter x for various values of the range a, again for fixed values of the other constants. The barrier heights are seen to decrease drastically with increasing range.

Figure 6 compares the calculated macroscopic contribution to the fission-barrier height with experimental values. The curve is calculated with the parameters of Eq. (10), and the experimental data represent both reduced fission-barrier heights for actinide nuclei [26,27] and shell-corrected fission-barrier heights for lighter nuclei [28]. In the region of fissility parameter x between 0.50 and 0.55 the experimental values are systematically somewhat higher than the calculated curve. It would be very desirable to have experimental data for still lighter nuclei with fissility parameter smaller than 0.5.

Figure 7 shows the difference between the predicted barrier height in the liquid-drop model with the parameter set from Ref. [3] and in our model with the parameters (10) along the line of beta-stability. The finite range of the nuclear force lowers the fission barriers of nuclei near silver by about 10 MeV relative to those calculated with the liquid-drop model and shifts the critical Businaro-Gallone point to $Z^2/A = 23$, in approximate agreement with recent experimental evidence [35].

7. POTENTIAL-ENERGY SURFACES OF LIGHT NUCLEI

The general trend to decrease the stiffness of nuclei with increasing range of the interaction a shows up especially for light nuclei where the radius is no longer an order of magnitude larger than a. A calculation of the deformation energy of ^{40}Ca as a function of the quadrupole deformation shows that the shell correction is more effective in producing a second minimum with our expression for the macroscopic part of the energy than with the conventional liquid-drop model, as seen in Fig. 8. This provides a natural interpretation of the rotational states observed in this nucleus and certain other light nuclei [37]. A similar study for ^{102}Zr shows that its calculated ground-state quadrupole moment is shifted somewhat towards larger values by the finite-range model, although it is still not as large as the experimentally observed quadrupole moment [38]. This result is shown in Fig. 9.

8. SUMMARY

We have redefined the surface term in the liquid-drop formula so that it can be used for configurations in which the size of a curvature radius of the nuclear surface becomes comparable to the surface thickness. We have shown that the new version of the liquid-drop formula yields a weaker dependence of the deformation energy on surface wiggles of high multipole order than the old model and generally results in a smaller nuclear stiffness. As a consequence the shell correction produces a larger ground-state deformation especially of some light nuclei, and there seems to appear a second minimum in the deformation-energy curve of ^{40}Ca.

Saddle-point shapes have been calculated, and they are less necked-in than in the usual liquid-drop model. The dependence of the Businaro-Gallone point on the range parameter of our model has been studied. We have derived an explicit expression for the nuclear interaction energy between two non-overlapping ions and have calculated interaction-barrier heights. For very heavy systems the maximum in the interaction energy transforms into a point of inflection and the interaction energy increases monotonically with decreasing distance between the ions.

We determined the parameters of our model so that the reduced fission barrier heights for fissility values larger than 0.5 and experimental interaction-barrier heights are reproduced on the average. The fission barriers for nuclei with a smaller fissility parameter are predicted to be lower than they are in the old version of the liquid-drop formula with parameters from Ref. [3].

ACKNOWLEDGMENTS

We are indebted to W. J. Swiatecki and W. D. Myers for suggestions and discussions throughout this work and to S. E. Koonin for writing the computer program to evaluate the three-dimensional integral for the nuclear macroscopic energy. We also thank J. Randrup for making his calculations available prior to publication.

REFERENCES

[1] BRACK, M., DAMGAARD, J., JENSEN, A.S., PAULI, H.C., STRUTINSKY, V.M., WONG, C.Y., Rev. Mod. Phys. 44 (1972) 320.
[2] MYERS, W.D., SWIATECKI, W.J., Nucl. Phys. 81 (1966) 1.
[3] MYERS, W.D., SWIATECKI, W.J., Ark. Fys. 36 (1967) 343.
[4] SEEGER, P.A., Atomic masses and fundamental constants (Proc. Fourth Conf. Teddington, 1971), Plenum, London (1972) 255.
[5] WONG, C.Y., Phys. Letters 41B (1972) 451.
[6] ABRAMOWITZ, M., STEGUN, I.A., Eds., Handbook of mathematical functions, National Bureau of Standards, Washington, D. C. (1964).
[7] TSANG, C.F., Berkeley Report, UCRL-18899 (1969).
[8] RANDRUP, J., SWIATECKI, W.J., to be published.
[9] MYERS, W.D., Berkeley Preprint, LBL-1259 (1972).
[10] BIMBOT, R., GAUVIN, H., LE BEYEC, Y., LEFORT, M., PORILE, N.T., TAMAIN, B., Nucl. Phys. A189 (1972) 539.
[11] GAUVIN, H., LE BEYEC, Y., LEFORT, M., DEPRUN, C., Phys. Rev. Letters 28 (1972) 697.
[12] LE BEYEC, Y., LEFORT, M., VIGNY, A., Phys. Rev. C 3 (1971) 1268.
[13] WONG, C.Y., Oak Ridge Preprint (1972).
[14] SIKKELAND, T., Ark. Fys. 36 (1967) 539.
[15] VIOLA, V.E., SIKKELAND, T., Phys. Rev. 128 (1962) 767.
[16] BIMBOT, R., GARDÈS, D., RIVET, M.F., Phys. Rev. C 4 (1971) 2180.
[17] BLANN, M., Bull. Am. Phys. Soc. 18 (1973) 31; slightly revised final values are given in GUTBROD, H.H., WINN, W.G., BLANN, M., Rochester Preprint, COO-3494-8 (1972).
[18] LE BEYEC, Y., LEFORT, M., SARDA, M., Nucl. Phys. A192 (1972) 405.
[19] LEFORT, M., NGÔ, C., PETER, J., TAMAIN, B., Nucl. Phys. A197 (1972) 485.
[20] OBST, A.W., MoSHAN, D.L., DAVIS, R.H., Phys. Rev. C 6 (1972) 1814.
[21] ORLOFF, J., DAEHNICK, W.W., Phys. Rev. C 3 (1971) 430.
[22] ROBERTSON, B.C., SAMPLE, J.T., GOOSMAN, D.R., NAGATANI, K., JONES, K.W., Phys. Rev. C 4 (1971) 2176.
[23] FLETCHER, N.R., WEST, L., KEMPER, K.W., Bull. Am. Phys. Soc. 16 (1971) 1149.
[24] BERTIN, M.C., TABOR, S.L., WATSON, B.A., EISEN, Y., GOLDRING, G., Nucl. Phys. A167 (1971) 216.
[25] GOLDRING, G., SAMUEL, M., WATSON, B.A., BERTIN, M.C., TABOR, S.L., Phys. Letters 32B (1970) 465.
[26] PAULI, H.C., LEDERGERBER, T., Nucl. Phys. A175 (1971) 545.
[27] RANDRUP, J., TSANG, C. F., MÖLLER, P., NILSSON, S. G., LARSSON, S. E., Berkeley Preprint (1973).
[28] MORETTO, L.G., THOMPSON, S.G., ROUTTI, J., GATTI, R.C., Phys. Letters 38B (1972) 471.
[29] GREEN, A.E.S., Nuclear Physics, McGraw-Hill, New York (1955) 185, 250.
[30] LÖBNER, K.E.G., VETTER, M., HÖNIG, V., Nucl. Data Tab. A7 (1970) 495.
[31] RAWITSCHER, G.H., Nucl. Phys. 85 (1966) 337.
[32] McINTYRE, J.A., BAKER, S.D., WANG, K.H., Phys. Rev. 125 (1962) 584.
[33] NIX, J.R., Nucl. Phys. A130 (1969) 241.
[34] BUSINARO, U.L., GALLONE, S., Nuovo Cim. 5 (1957) 315.
[35] METHASIRI, T., JOHANSSON, S.A.E., Nucl. Phys. A167 (1971) 97.
[36] MÖLLER, P., NIX, J.R., Paper IAEA-SM-174/202, these proceedings.
[37] SETH, K.K., SAHA, A., GREENWOOD, L., Northwestern University Preprint (1973).
[38] CHEIFETZ, E , JARED, R.C., THOMPSON, S.G., WILHELM, J.B., Phys. Rev. Letters 25 (1970) 38.
[39] BOLSTERLI, M., FISET, E.O., NIX, J.R., NORTON, J.L., Phys. Rev. C 5 (1972) 1050.

FIGURE CAPTIONS

Fig. 1. Contour diagram of the effective nuclear radius parameter r_{eff} as a function of the charge numbers of the colliding ions for nuclei along the valley of beta-stability (defined by Green's formula $N-Z = 0.4\ A^2/(A+200)$; see Ref. [29]).

Fig. 2. Contour diagram of the distance d between the equivalent sharp surfaces of two spherical nuclei of charges Z_1 and Z_2 at the peak of the interaction potential. The results are for nuclei along the valley of beta-stability. Beyond the line defined by d = 0 the interaction barrier has no maximum.

Fig. 3. Comparison of experimental and calculated interaction barrier heights. The solid points are experimental values derived from excitation functions (solid circle [10], solid square [11], solid diamond [12], solid upward-pointing triangle [13,14], solid downward-pointing triangle [13,15], solid hexagon [16], solid plus sign [17], and solid star [18]); the open points are experimental values derived from elastic-scattering data (open circle [19], open square [20], open diamond [20,21], open upward-pointing triangle [20,22], open downward-pointing triangle [20,23], open hexagon [20,24], open plus sign [24], and open star [25]).

Fig. 4. Saddle-point shapes as functions of the fissility parameter $x=E_c^{(0)}/[2E_s^{(0)}]$ for liquid-drop-model parameters from Ref. [3] and $a/r_0 = 0.0(0.2)1.2$. The upper portion of the diagram gives the largest radius of the saddle-point shape in units of the radius of the sphere with equal volume. The lower portion gives the smallest radius. The solid points give the location of the Businaro-Gallone point.

Fig. 5. Fission-barrier height in our model as a function of the fissility parameter x and the range a/r_0 for liquid-drop-model parameters from Ref. [3]. The solid points mark the Businaro-Gallone point.

Fig. 6. Comparison of theoretical fission-barrier heights (solid line) calculated with the parameters (10) and experimental barrier heights corrected for single-particle effects. The circles [26] and squares [27] are reduced fission-barrier heights for actinide nuclei, and the triangles [28] are shell-corrected fission-barrier heights for lighter nuclei.

Fig. 7. Comparison of macroscopic barrier heights calculated in our model with the parameters (10) and in the liquid-drop model with parameters from Ref. [3] for nuclei along the line of beta-stability. The solid points indicate the Businaro-Gallone point. The arrows show the mass numbers at which the system would lose stability towards fission if shell corrections were not present.

Fig. 8. Deformation energy of ^{40}Ca. The dashed lines show the macroscopic contribution to the deformation energy in our model and in the conventional liquid-drop-model. The solid curves give the total deformation energy including single-particle corrections; these corrections are calculated by use of the methods and parameters of Ref. [36].

Fig. 9. Analogous diagram to Fig. 8 for ^{102}Zr; the single-particle corrections are calculated by use of the methods and parameters of Ref. [39].

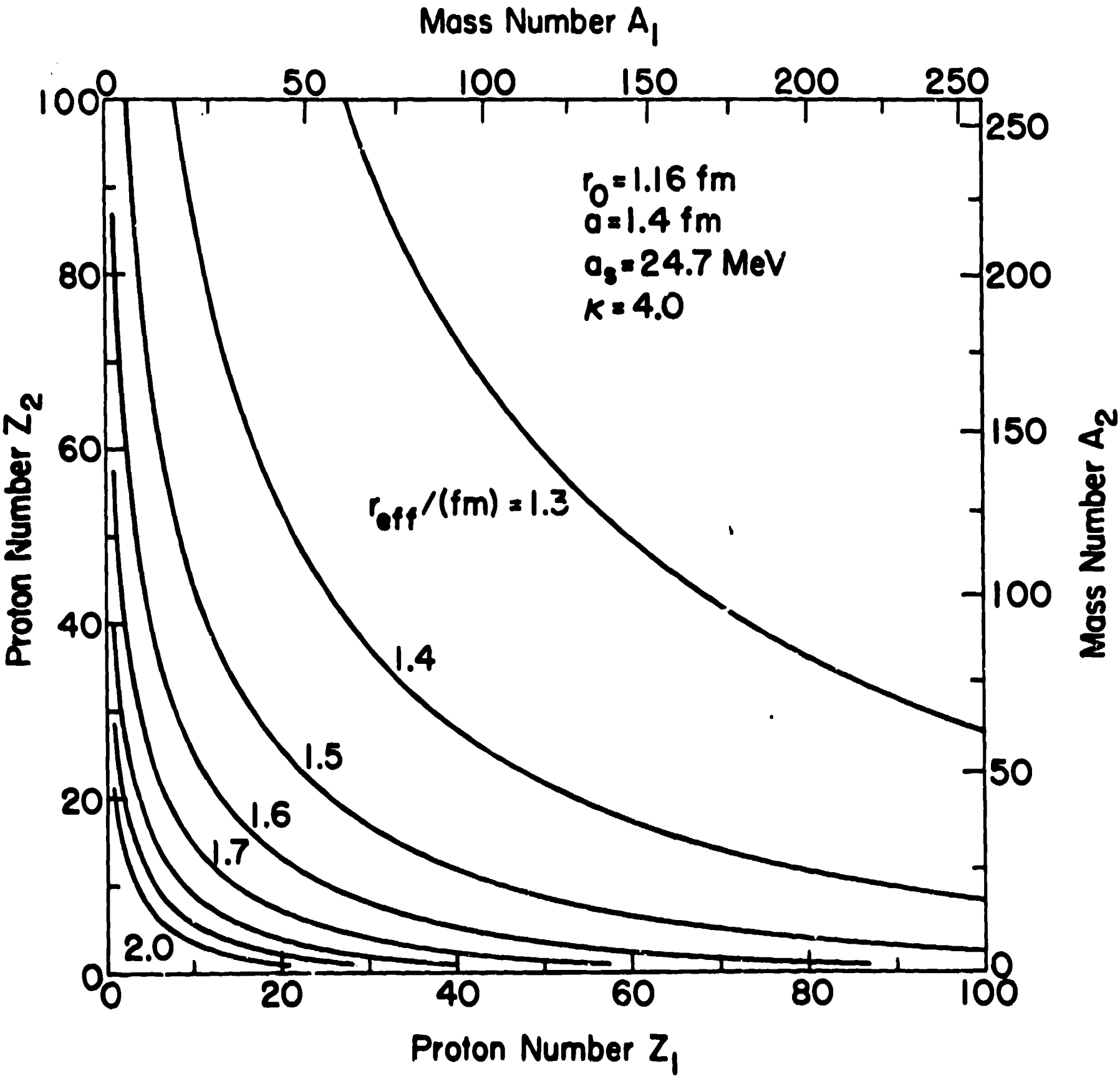

Figure 1

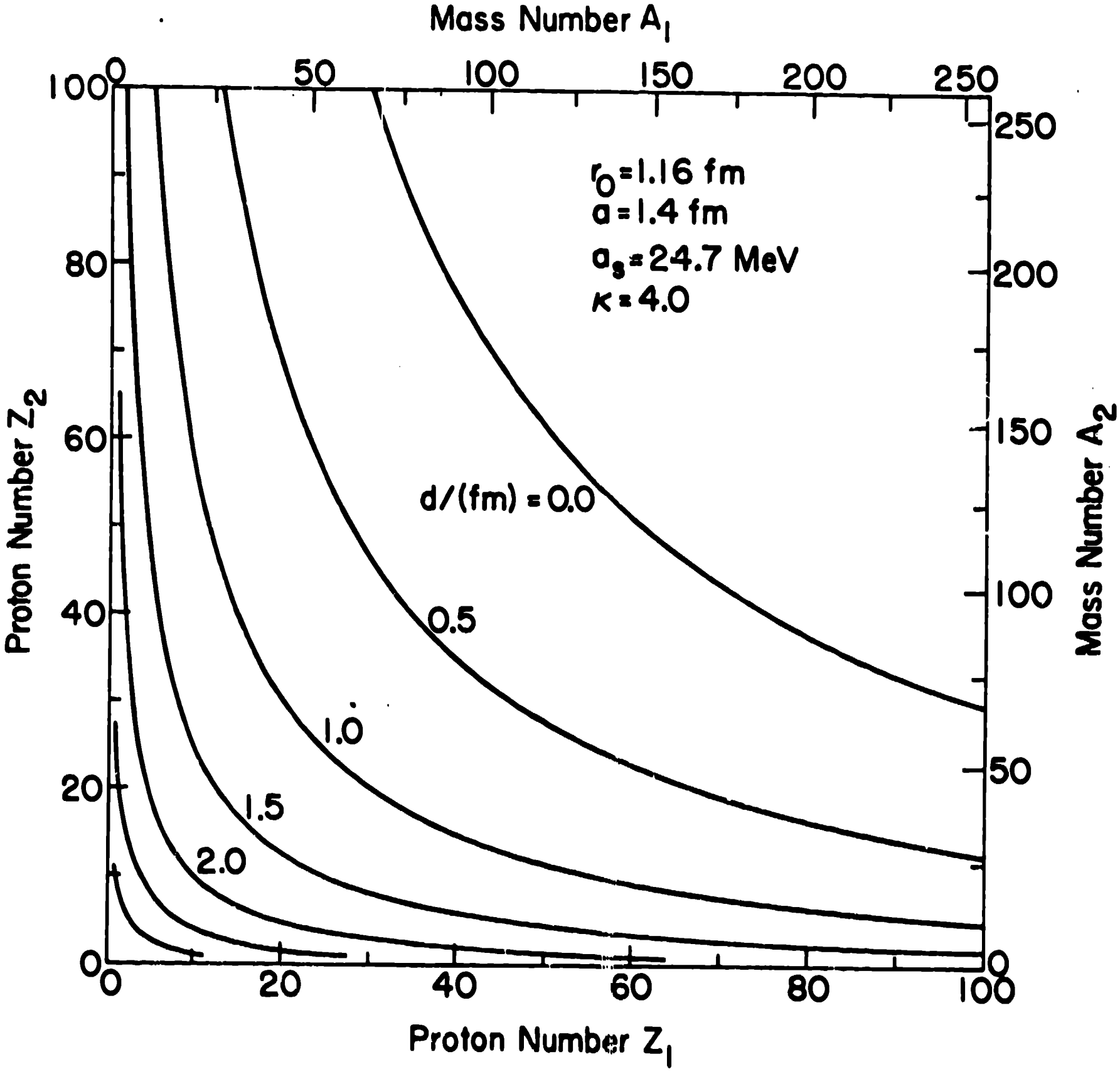

Figure 2

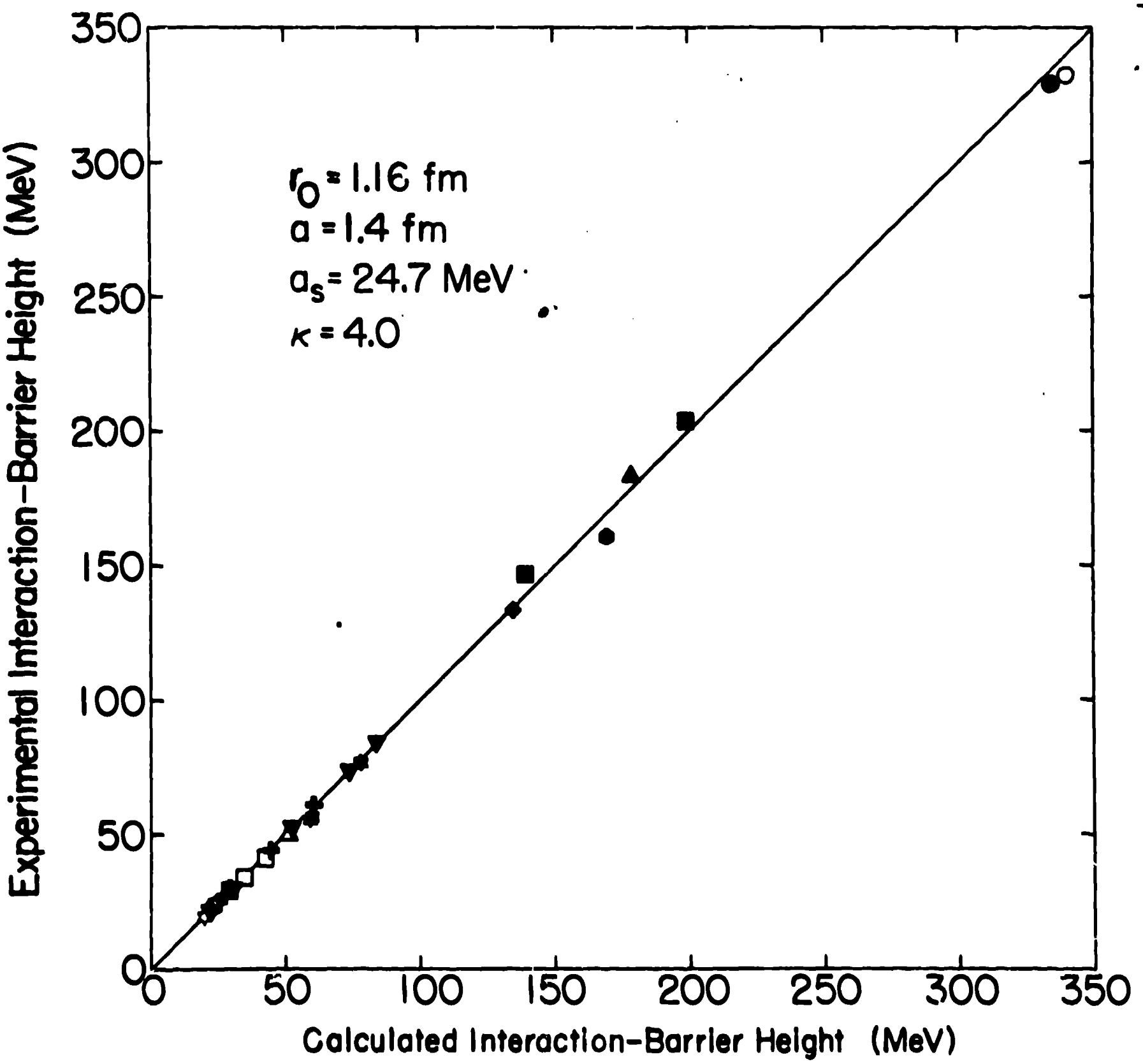

Figure 3

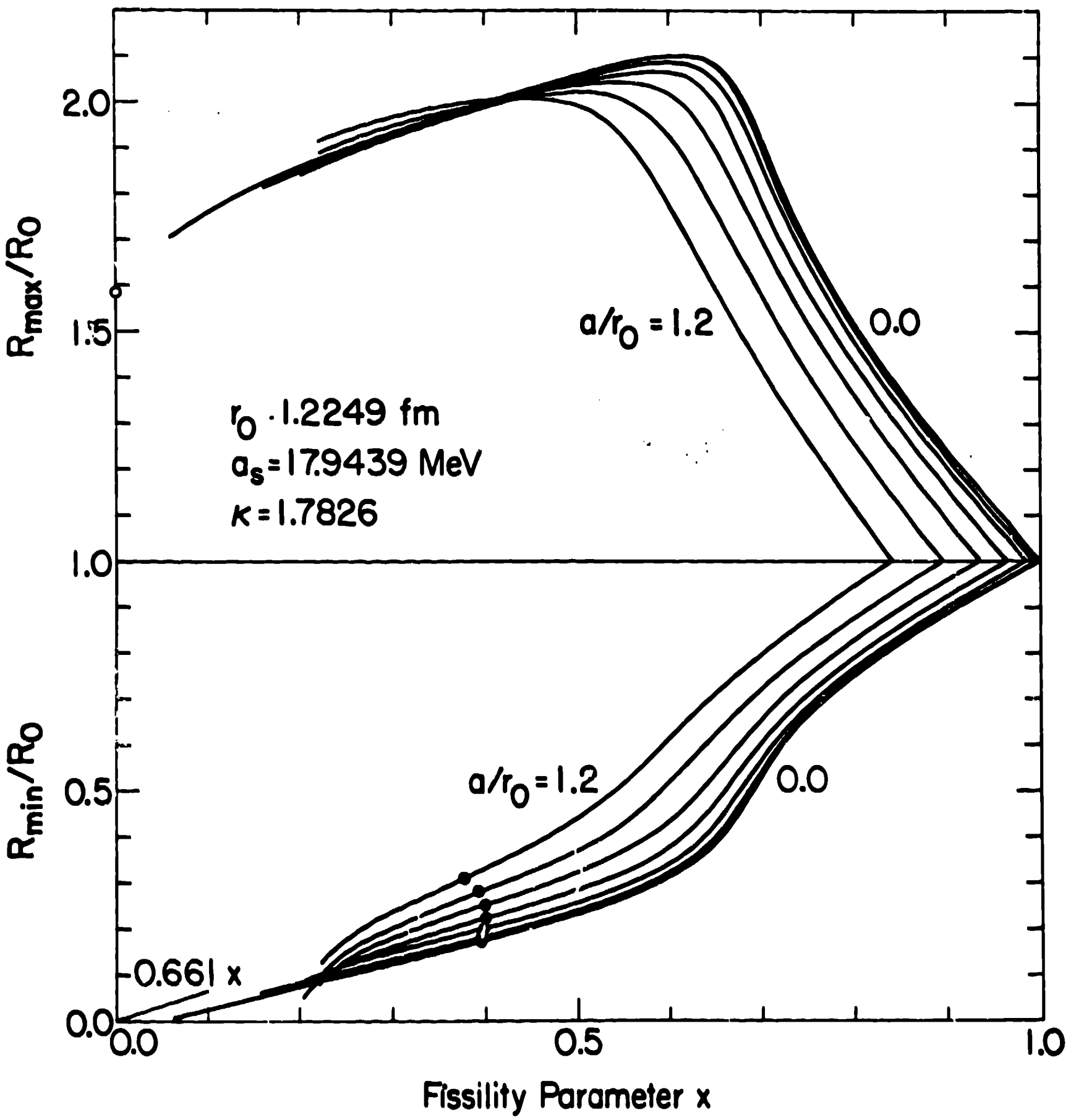

Figure 4

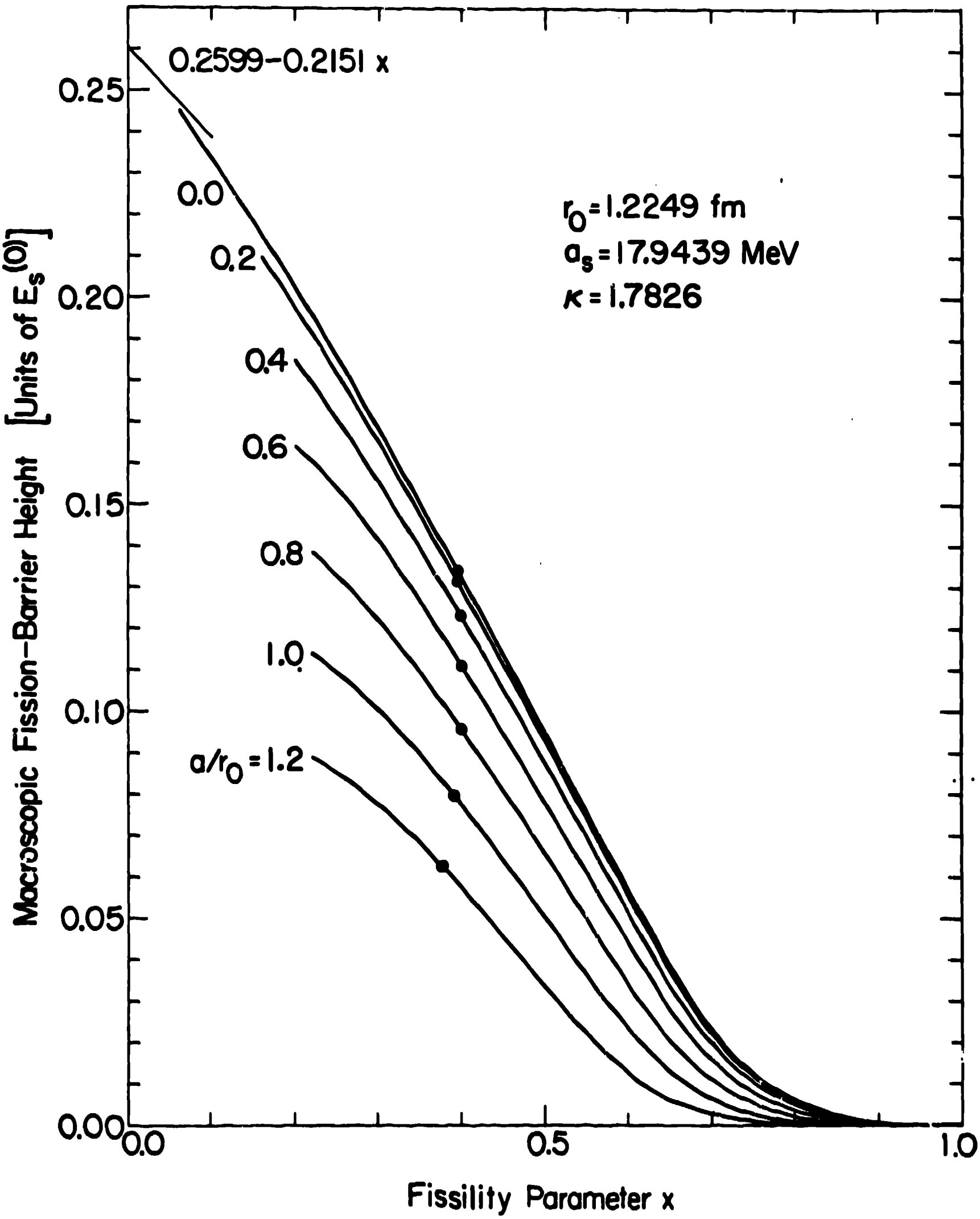
0.2599-0.2151 x
0.0
0.2
0.4
0.6
0.8
1.0
a/r0 = 1.2
r0 = 1.2249 fm
as = 17.9439 MeV
κ = 1.7826
Macroscopic Fission-Barrier Height [Units of Es(0)]
0.25
0.20
0.15
0.10
0.05
0.00
0.0
0.5
1.0
Fissility Parameter x

Figure 5

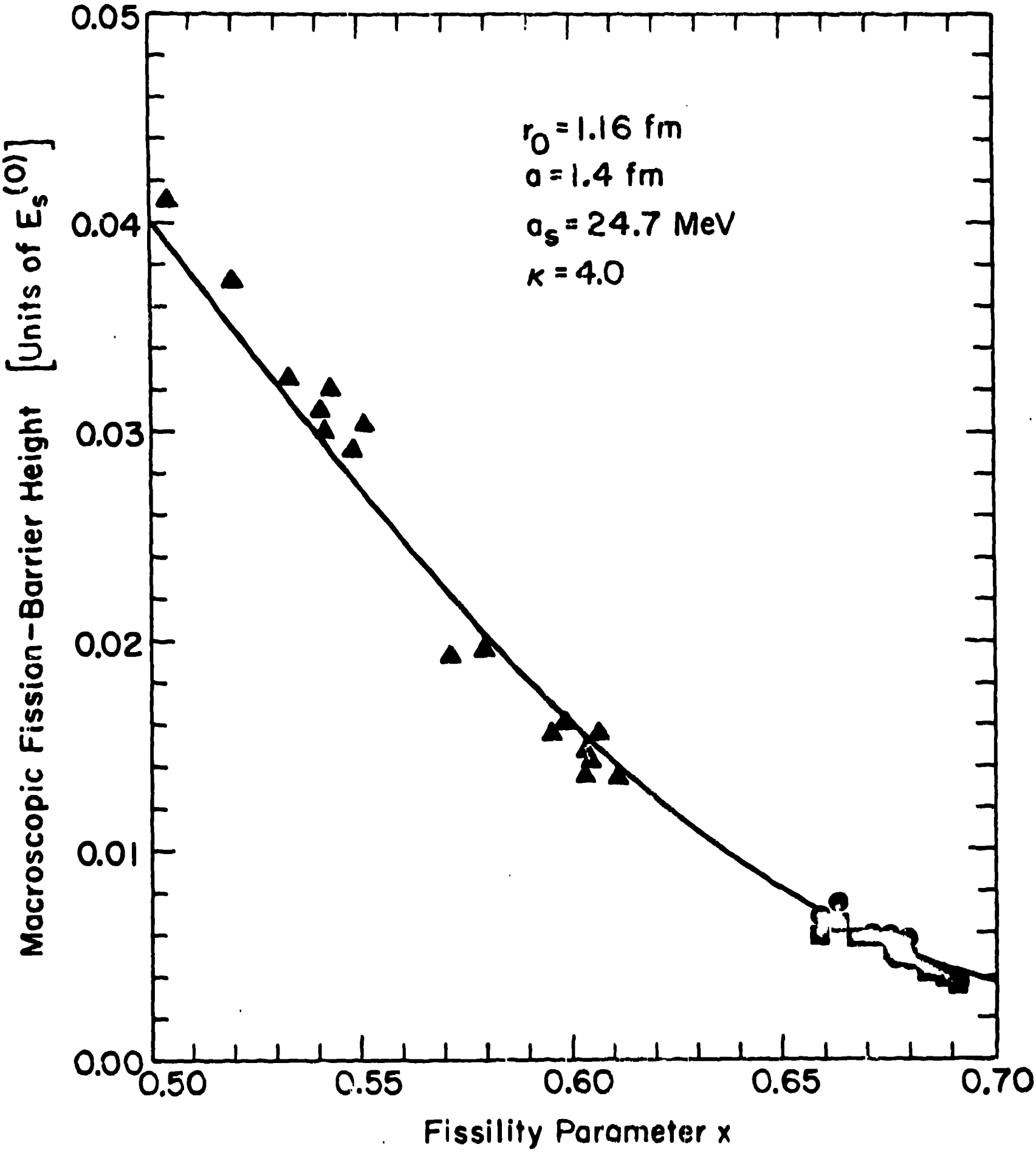
0.05
0.04
0.03
0.02
0.01
0.00
0.50
0.55
0.60
0.65
0.70
$r_0 = 1.16$ fm
$a = 1.4$ fm
$a_s = 24.7$ MeV
$\kappa = 4.0$
Macroscopic Fission-Barrier Height [Units of $E_s^{(0)}$]
Fissility Parameter x

Figure 6

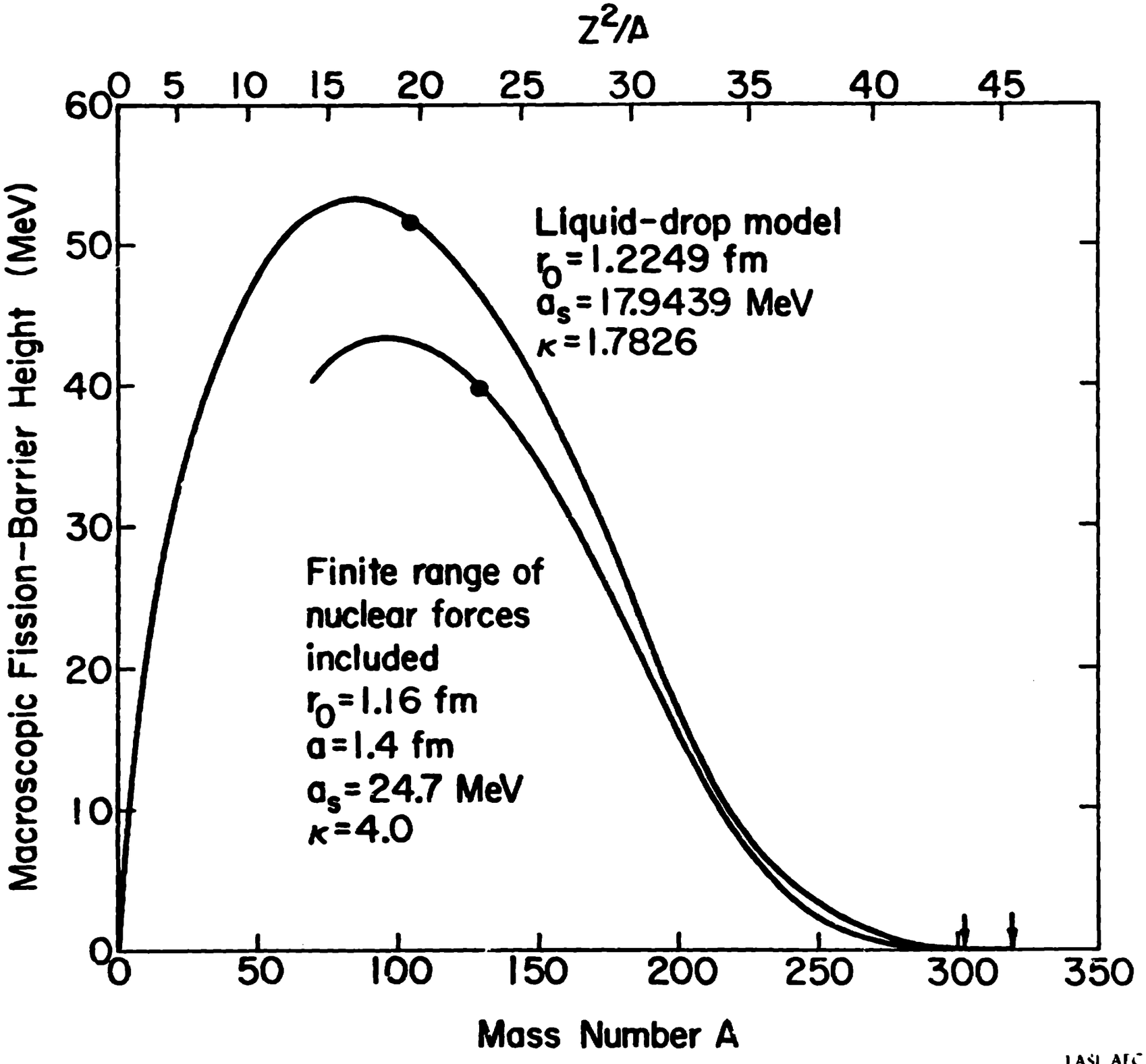

Figure 7

LASL AEC OFFICIAL

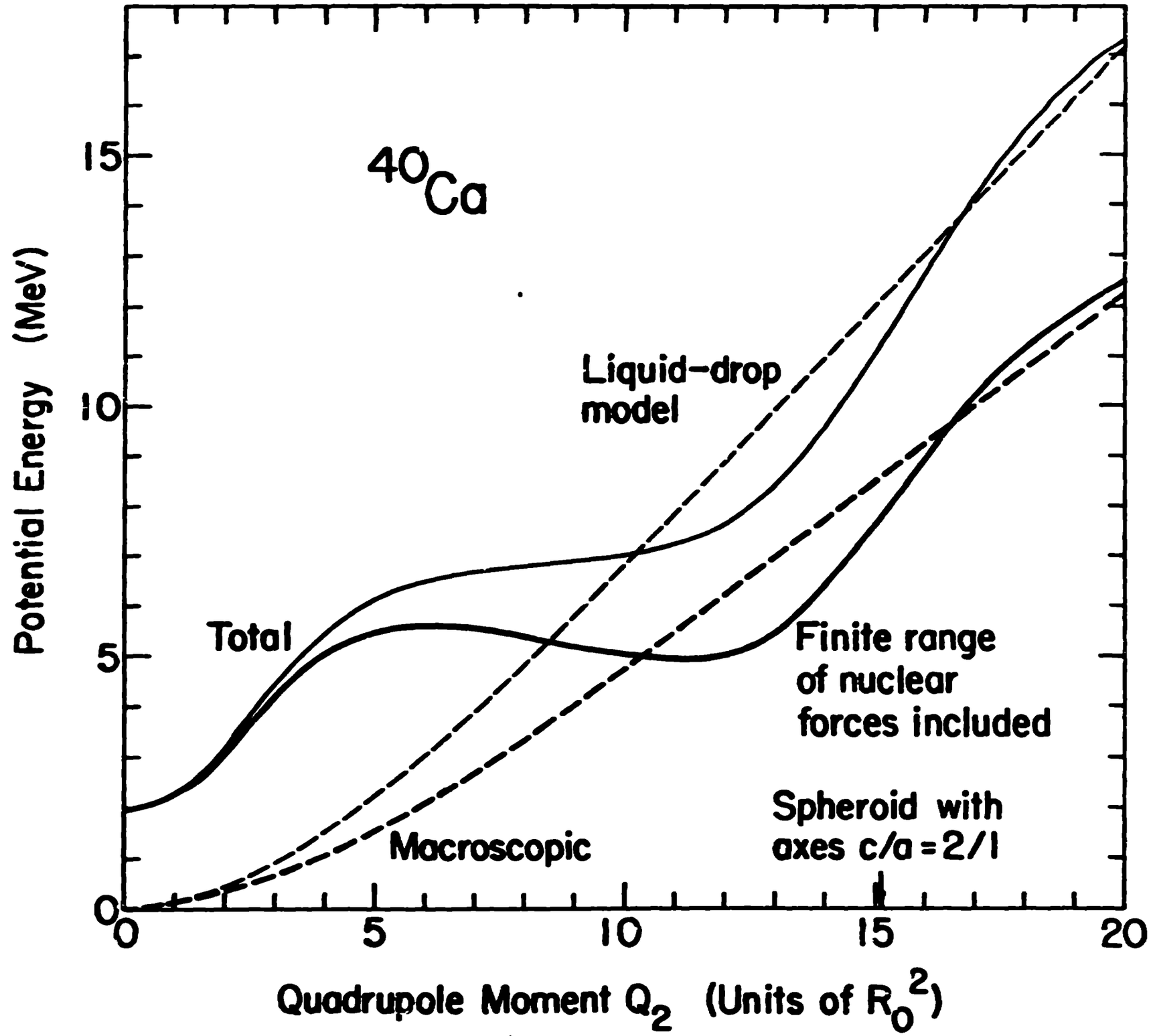

Figure 8

LASL AEC OFFICIAL

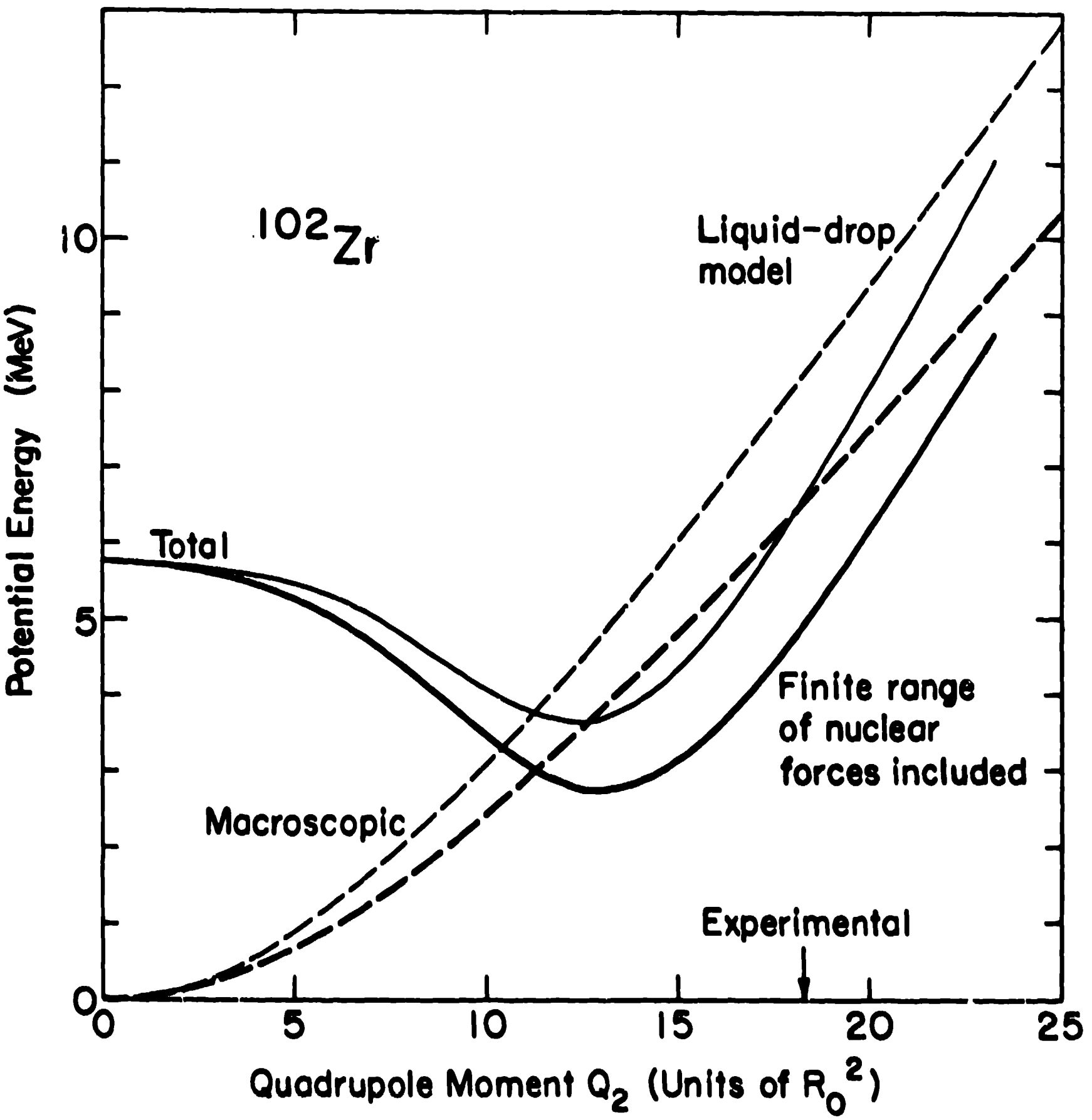

Figure 9